

SNR improvement of MST Radar signals using sparse signal recovery algorithm

Raju C^{1*}, Sreenivasulu Reddy T²

^{1,2} Department of ECE, Sri Venkateswara University College of Engineering,

Tirupati

(*E-mail: c.raju1112@gmail.com)

Abstract— Wind profiling radars, known as MST (Mesosphere Stratosphere Troposphere) Radars, conceived as a technology to provide wind profiles in the upper atmosphere with a much better temporal resolution than radiosonde. The Radar wind profiler is most suitable remote sensing tool for measuring the height profile of wind vector with high resolutions in both time and space in all weather conditions. The term wind profiling radar is often used to emphasize the operational applications of the clear air radar technique and operating at lower and middle UHF bands. Signal processing of this MST radar is necessary to estimate the wind profiler moments and signal to noise ratio (SNR). The signals, which are processed in the present work has been obtained from the MST Radar at National Atmospheric Research Laboratory (NARL), Gadanki, India. SNR computation is an important parameter in signal processing. This paper discusses improvement of SNR using sparse signal recovery algorithm. Results show that there is a significant improvement in SNR values even at higher range bins of radar data.

Keywords— MST Radar, SNR, sparse signals, Radiosonde.

I. INTRODUCTION

RADAR is the short form for Radio Detection and Ranging. Radar can be used, in addition to the detection and characterization of hard targets, to probe the soft or distributed targets such as the earth's atmosphere. The principle of operation of radar is that whenever a pulse of EM (electromagnetic) wave is broadcasted towards a distantly located target or object, a portion of the energy is getting back giving information about it, through reflection or dispersion. The time delay between the pulse transmitted and pulse received will provide the range. These types of radars are called as pulse radar. The pulse Doppler radars have the capability of detecting the target, even when it is in motion. The echo is the Doppler shift from the transmitted and the shift gives the line-of-sight velocity of the object. By knowing the angular position of the target, the location is determined uniquely. Such radars utilize large antennas of either phased array or dish type for transmission and reception to produce narrow beams. The significant parameters that distinguish the potential of the radar are resolution and sensitivity. The resolution depends on the pulse length and beam width whereas the sensitivity of the radar depends on the peak power-aperture product. Various types of pulse radars have

been developed to meet the demands of application in diverse fields.

The Atmospheric radars of interest to the present study are called as clear air radars and they operate typically in the Very High Frequency (VHF) (30 –300 MHz) and Ultra High Frequency (UHF) (300 MHz – 3GHz) bands [1]. The target for clear air radars are the turbulent fluctuations in the refractive index on the atmosphere. The other class of radars called weather radars that serve to monitor the weather systems and they typically work in Super High Frequency band (SHF) (3-30 GHz) [2]. The revolutionary work of Woodman and Guillen (1974) led to the investigation of the Mesosphere-Stratosphere-Troposphere (MST) domain by employing a high power VHF backscatter operating ideally around 50 MHz.

II. THE INDIAN MST RADAR

The National MST Radar Facility (NMRF) has been established at Gadanki (13.5°N, 79.2°E), near Tirupati, India is an exceptional system used for atmospheric probing in the regions of Mesosphere, Stratosphere and Troposphere (MST) covering up to a height of about 100 Km. The study of ionosphere is also possible by the coherent backscattered echo. The study of various dynamical processes in the atmosphere can be done by examining the data collected from the MST radar. It is the state of art instrument that is capable of giving the parameters of atmosphere like wind speed, temperature, humidity etc.

The operational frequency of the radar is 53 MHz with $3 \times 10^{10} \text{ Wm}^2$ of peak power aperture product. The atmospheric study, waves, turbulence are studied from the echo received by the MST radar. Echoes below 50 km arise primarily due to neutral turbulence whereas above 50 km, the echoes are due to irregularities in the electron density. In the height range 30-60 km, density of the atmosphere as well as electron density is very low resulting in very weak echoes resulting in a gap region in most of the MST radars. The block diagram of MST radar located at Gadanki is shown in Fig 1.

MST radar data is processed in online and offline stages. The data is compressed significantly in online processing by averaging the time samples which generates power spectra. The extraction of parameter is done through

offline mode. The complex radar data is decoded and coherent integrations are performed. This preprocessed radar data is given as the input to the data processing system. The coherent integration filters out much of the wide band noise and decreases the volume of the data to the processor. The signal detectability is increased by integrating the detected quadrature signals over a time period [3]. Then Fast Fourier Transform (FFT) is performed to the complex time series of the data samples. The Doppler power spectrum for each range bin of the selected range window is computed through online mode. The Atmospheric Data Processor (ADP) is used for the parameterization of the Doppler spectrum [4].

learning, and signal processing (e.g., DOA estimation, power spectral estimation, channel estimation in communications, image restoration, biomedical, satellite imaging, etc.). The standard data model for sparse signal recovery algorithm is given by

Let the received signal sequence can be modeled as

$$\mathbf{y} = \mathbf{A}\mathbf{x} + \mathbf{q} \tag{1}$$

where $\mathbf{y} = [y_1, y_2, \dots, y_N]^T$ and $\mathbf{q} = [q_1, q_2, \dots, q_N]^T$,
 $\mathbf{A} = [\mathbf{a}(\omega_1) \ \mathbf{a}(\omega_2) \ \dots \ \mathbf{a}(\omega_K)]$ with
 $\mathbf{a}(\omega_k) = [a_1(\omega_k) \ \dots \ a_N(\omega_k)]^T$, $a_n(\omega_k) = \exp(jn\omega_k)$, $\omega_k = 2\pi(k-1)/K$; $k = 1, 2, \dots, K$

$\mathbf{x} = [x_1, x_2, \dots, x_K]^T$ with $K > N$. The fractional lower-order moment of q_n is denoted by $\sigma_n = \sigma$, for $n = 1, 2, \dots, N$.

The cost function of Sparse recovery algorithm namely Sparse Learning via Iterative minimization (SLIM) [5] is

$$J = K \log(\sigma) + \frac{1}{\sigma} \|\mathbf{y} - \mathbf{A}\mathbf{x}\|_2^2 + \sum_{k=1}^K \frac{2}{c} (|x_k|^c - 1) \tag{2}$$

where c is the controlling parameter. Here, c is put to 0 and the term $\sum_{k=1}^K \frac{2}{c} (|x_k|^c - 1)$ turned into $2 \sum_{k=1}^K \log(|x_k|)$.

The equation is minimized with respect to \mathbf{x} :

$$\nabla J = -\frac{1}{\sigma} \mathbf{A}^H (\mathbf{y} - \mathbf{A}\mathbf{x}) + \text{diag}(|x_1|^{-2} \ |x_2|^{-2} \ \dots \ |x_K|^{-2}) \mathbf{x} \tag{3}$$

Then $\nabla J = 0$ yields the estimate \hat{x}_k in each iteration [6,7]

$$\hat{x}_k(l+1) = |\hat{x}_k(l)|^2 (\mathbf{a}^H(\omega_k(\mathbf{P}(l))^{-1} \mathbf{y})); k = 1, 2, \dots, K \tag{4}$$

and similarly

$$\hat{\sigma}(l+1) = \frac{1}{N} \|\mathbf{y} - \mathbf{A}\hat{\mathbf{x}}(l+1)\|_2^2 \tag{5}$$

where

$$\mathbf{P}(l) = \mathbf{A} \text{diag}(|x_1(l)|^2 \ |x_2(l)|^2 \ \dots \ |x_3(l)|^2) \mathbf{A}^H + \hat{\sigma}(l) \mathbf{I}_N \tag{6}$$

The number of multiplications for the algorithm is $\mathcal{O}(KN^2 + N^3)$.

The steps involved in the algorithm are

1. Initialize the values of $\{\hat{x}_k(l)\}$ using the discrete Fourier transform
2. Update $\hat{\sigma}(l)$ using (5)
3. Update $\hat{x}_k(l+1)$ according to (4)
4. Repeat steps 2 and 3 until the convergence condition is satisfied.

IV RESULTS

The data collected from the MST radar located at Gadanki, Andhra Pradesh, India is used for the current study. The data collected is processed through the ADP which is represented as EALG (Existing Algorithm) and sparse recovery algorithm which is represented as PALG (proposed algorithm).

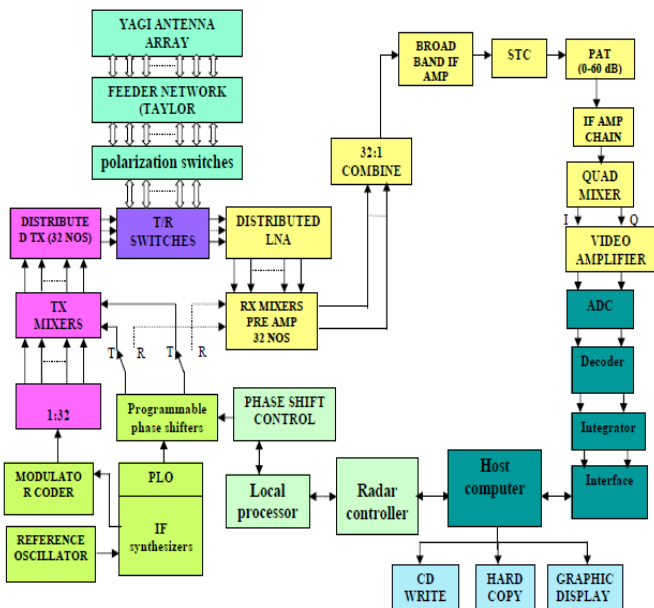


Fig. 1 Functional block diagram of Indian MST radar



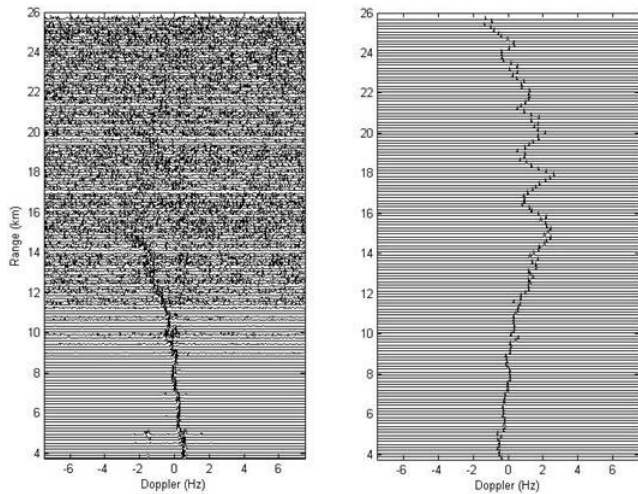
Fig. 2 Photograph of the MST radar antenna array located at Gadanki.

[courtesy:Director, National MST Radar Facility (NMRF)]

III. SPARSE SIGNAL RECOVERY ALGORITHM

To reconstruct a sparse signal vector from a restricted number of measurements has drawn attention from investigators from various fields, including mathematics, statistics, machine

The distinctive spectra of the radar data collected on Feb 9, 2015, for east beam before and after denoising are depicted in the Fig. 3.



g. 3 Distinctive Spectra of the radar data collected on Feb 9, 2015

(East beam) (A) before Denoising (B) after Denoising

The output SNR estimated from power spectrum obtained using EALG and PALG for the east and west beam for the radar data retrieved on Feb 9, 2015 is shown in Fig. 4. The figure is depicted from 11 to 22 Km only as more noise is seen in higher altitudes. The Fig. 5 represents the height profiles of the SNR estimated for the north and south beams. From both figures, it is evident that the PALG gives more signal-to-noise ratio even at higher range bins that maximizing the signal detectability of the radar. The output SNR is obtained using the method proposed in Hilderband and Sekhon [8].

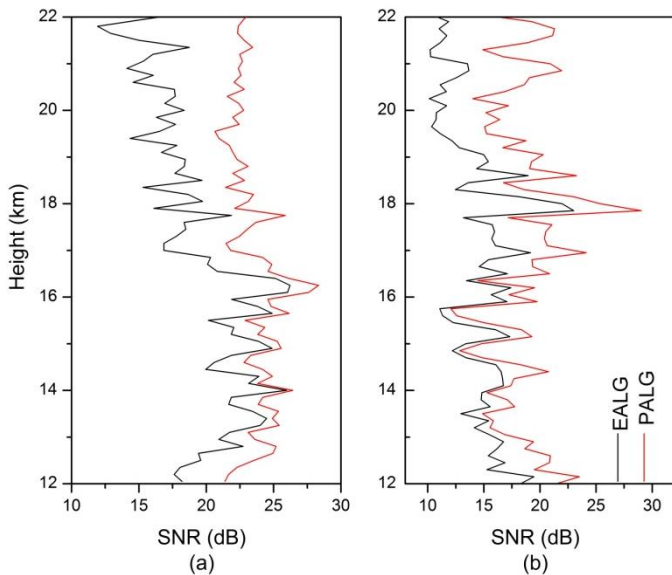


Fig. 4 Height Profiles of SNR Estimated Using EALG and PALG for East and West beams for data collected on Feb 9, 2015.

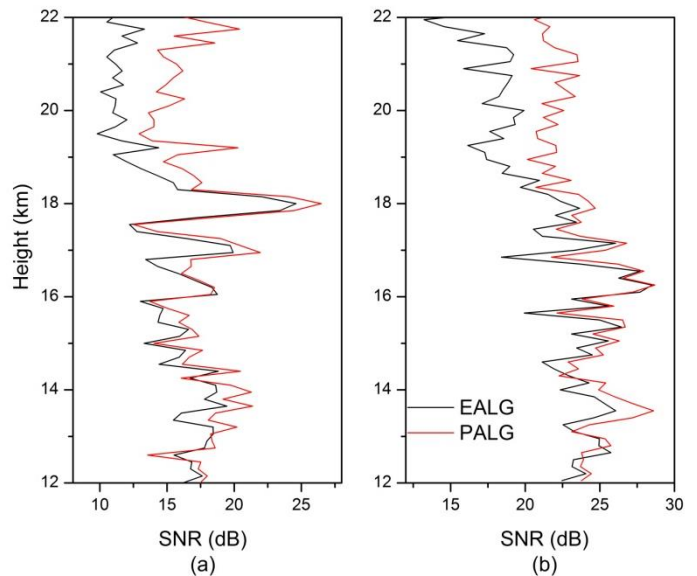


Fig. 5 Height Profiles of SNR Estimated Using EALG and PALG for North and South beams for data collected on Feb 9, 2015.

The comparison of average SNR values in dB for four beams on February 9 and 10, 2015 for the EALG and PALG is given in Table 1. From Table 1, it is seen that PALG gives the better enhancement in average SNR values over the EALG.

Table 1. Comparison of Average SNR for EALG and PALG

Date	Algorithm	East	West	South	North
Feb 9, 2015	EALG	19.47	18.23	21.57	20.14
	PALG	23.96	23.17	24.28	22.82
Feb 10, 2015	EALG	22.35	23.41	17.86	18.56
	PALG	25.61	23.98	18.94	20.31

V. CONCLUSION

In this paper, a sparse recovery algorithm has been presented to improve the signal to noise ratio for the MST Radar data. There is a significant improvement in the SNR values even at higher range bins. The detectability of the signal is increased. Various norms can be used for the better spectral estimation and further improvement in SNR values. The complexity of the algorithm can be further reduced by incorporating some efficient techniques for the computation of the covariance matrix.

ACKNOWLEDGMENTS

The authors are very thankful to National Atmospheric Research Laboratory (NARL), Gadanki for providing radar data and Centre of Excellence, Department of ECE, SV University College of Engineering for technical assistance.

REFERENCES

- [1] Rötteger, J., and M.F. Larsen, UHF/VHF Radar techniques for atmospheric research and wind profiler applications, in Radar in Meteorology, edited by D. Atlas, chap. 21a, pp 235-281, American Meteorological Society, Boston, Mass., 1990.
- [2] Doviak, R.J., and Zrnic.D.S, Doppler radar and Weather Observations, Academic Press, London 1984.
- [3] Farley, D.T., On-line data processing techniques for MST radars, Vol 20, No.6, Pp 1177-1184, 1985.
- [4] V. K. Anandan, Atmospheric Data Processor-Technical and User Reference Manual. NMRF, DOS Publication, Gadanki, 2001.
- [5] Xing Tan, William Roberts, Jian Li, Petre Stoica, "Sparse Learning via Iterative Minimization With Application to MIMO Radar Imaging," *IEEE Trans. Signal Process.*, 2011, 1088-1101.
- [6] Duc Vu, Luzhou Xu, Ming Xue, Jian Li, "Nonparametric Missing Sample Spectral Analysis and Its Applications to Interrupted SAR," *IEEE J. Sel. Topics Signal Process.*, 2012, 1-13.
- [7] P. Stoica and Y. Selén, "Cyclic minimizers, majorization techniques, and expectation-maximization algorithm: A refresher," *IEEE Signal Process. Mag.*, vol. 21, no. 1, pp. 112–114, Jan. 2004.
- [8] P. H. Hildebrand and R. Sekhon, "Objective determination of the noise level in Doppler spectra," *Journal of Applied Meteorology*, vol. 13, no. 7, pp. 808–811, Oct. 1974.
- [9] T. S. Reddy and G. R. Reddy, "Spectral analysis of atmospheric radar signal using filter banks polyphase approach," *Digital Signal Processing*, 2010; 20, No. 4, 1061– 1071.
- [10] S. Thatiparthi, R. Gudheti, and V. Sourirajan, "MST radar signal processing using wavelet-based denoising," *IEEE Geoscience Remote Sensing Letters*, 2009; 6, No. 4, 752-756.
- [11] T. S. Reddy and G. R. Reddy, "MST radar signal processing using cepstral Thresholding," *IEEE Transactions on Geoscience and Remote Sensing*, 2010; 48, No. 6, 2704-2710.
- [12] Neetha I. Eappen, T. Sreenivasulu Reddy, and G. Ramachandra Reddy, "Semiparametric algorithm for processing MST Radar data," *IEEE Transactions on Geoscience and Remote Sensing*, Vol: 54, No. 5, pp. 2713-2721, May 2016.